Inorganic Chemistry

Article

pubs.acs.org/IC

Synthesis and Characterization of Novel Wells–Dawson-Type Mono Vanadium(V)-Substituted Tungsto-polyoxometalate Isomers: 1- and 4-$[S_2VW_{17}O_{62}]^{5-}$

Tadaharu Ueda,*[,†] Miho Ohnishi,[†] Motoo Shiro,[‡] Jun-ichi Nambu,[†] Toshiaki Yonemura,[†] John F. Boas,[§] and Alan M. Bond[∥]

[†]Department of Applied Science, Faculty of Science, Kochi University, Kochi 780-8520, Japan

[‡]X-ray Research Laboratory, Rigaku Corporation, Akishima, Tokyo 196-8666, Japan

[§]School of Physics, Monash University, Clayton, Victoria 3800, Australia

[∥]School of Chemistry, Monash University, Clayton, Victoria 3800, Australia

Supporting Information

ABSTRACT: Two vanadium(V)-substituted tungsto-polyoxometalate isomers, 1- and 4-$[S_2VW_{17}O_{62}]^{5-}$, were prepared as their tetra-alkyl ammonium salts from a W^{VI}–H_2SO_4–V^V reaction mixture in aqueous CH_3CN solution. X-ray crystallographic structural analysis revealed that both isomers have a Wells–Dawson-type structure with a higher occupancy of vanadium at polar sites and belt sites for 1- and 4-$[S_2VW_{17}O_{62}]^{5-}$, respectively. The isomers were also characterized by elemental analysis, infrared, Raman, UV–vis, and ^{51}V NMR spectroscopies as well as voltammetry, and the data obtained were compared with that derived from $[S_2W_{18}O_{62}]^{4-}$. Significantly, the reversible potentials for the vanadium(V/IV) couple for both 1- and 4-$[S_2VW_{17}O_{62}]^{5-}$ in CH_3CN (0.1 M n-Bu_4NPF_6) are considerably more positive than the tungstate reduction process exhibited by the $[S_2W_{18}O_{62}]^{4-}$ framework, implying that the presence of vanadium should be useful in catalytic reactions. The one-electron-reduced $[S_2V^{IV}W_{17}O_{62}]^{6-}$ forms of both isomers were prepared in solution by controlled potential bulk electrolysis and characterized by voltammetry and EPR spectroscopy.

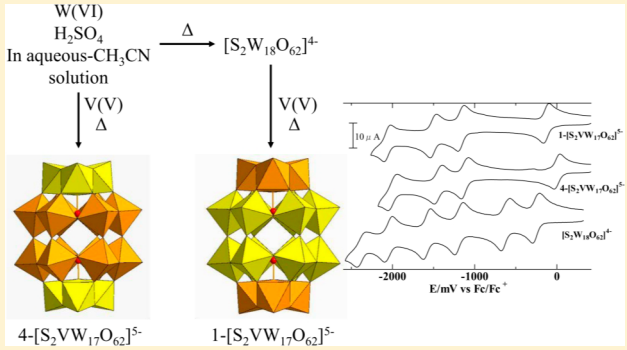

INTRODUCTION

Polyoxometalates have been extensively studied for a long period of time because of their practical applications in catalysis, analytical chemistry, biochemistry, and other fields.[1−4] Recently, interest also has been focused on their use in a green chemistry context as environmentally friendly catalysts.[5−11] They also are of substantial fundamental interest because of their wide variety of chemical and physical properties that depend on their elemental components, structures, redox level, and anion charge.

The framework of many polyoxometalates is constructed from oxo-molybdenum and oxo-tungsten units. However, it is common for the W and Mo metals in the oxo unit to be replaced by other metals to form metal-substituted polyoxometalates that are often prepared by reaction of the relevant combination of lacunary polyoxometalate and metal ion at an appropriate pH.[1,12] These substituted polyoxometalates exhibit a wide range of structures that are often of the Keggin- and Wells–Dawson-type.[1−4] The metal-substituted polyoxometalates often exhibit interesting new chemical properties, including selective catalysis and unique redox chemistry that depend on the identity of the substituted metal.[1−4,13] Of particular relevance to this present study, vanadium-substituted polyoxometalates have been shown to be excellent catalysts for facilitation of oxidation reactions in organic syntheses.[5−11,14]

Polyoxometalates usually also contain a hetero ion in a central position within the framework.[15] The most widely studied ones have used silicate or phosphate for this purpose. Other hetero ions, such as germanate, arsenate, or sulfate, have been introduced into the central position. In the case of sulfate, the Keggin- and Wells–Dawson-type polyoxometalates, $[SM_{12}O_{40}]^{2-}$ and $[S_2M_{18}O_{62}]^{4-}$ (S_2M_{18}; M = Mo, W) have been synthesized from reactions undertaken in mixed aqueous–organic solvent media,[16,17] with $[S_2M_{18}O_{62}]^{4-}$ being photocatalytically active. Vanadium(V) ions have been incorporated into the central position as a vanadate anion and also in the framework part of the polyoxometalate.[18] Unlike the case with other metal ions, the vanadium(V) ion can be substituted into a molybdenum and tungsten polyoxometalate without creating defect sites.[19] In the case of the Keggin-type polyoxometalates, Ueda et al.[20] showed that the permittivity of the organic solvent used in the reaction medium plays a key role in determining the outcome of the

Received: December 4, 2013
Published: April 30, 2014

   dx.doi.org/10.1021/ic402994q | Inorg. Chem. 2014, 53, 4891−4898

vanadium substitution reaction. In the Wells–Dawson class, $(n\text{-}Bu_4N)_5[S_2VMo_{17}O_{62}]$ has been prepared from an aqueous–organic mixed solvent,[21] but vanadium-substituted tungstosulfates are not yet known. Vanadium-substituted polyoxometalates of the $[XVM_{11}O_{40}]^{4-}$ (XVM_{11}; X=P, As; M = Mo, W) and $[XVW_{17}O_{62}]^{7-}$ (X_2VW_{17}) classes are relatively common and much more easily reduced electrochemically than their parent forms, XM_{12} and X_2W_{18}, respectively. On this basis, it is expected that vanadium substitution in S_2W_{18}, achieved for the first time in this study, also would lead to substantial positive shifts in reversible potentials and would modify their photocatalytic and other properties. With the goal of achieving controlled modifications in the characteristics of the S_2W_{18} class of polyoxometalates, we now report the preparation of $n\text{-}Bu_4N^+$ salts of two vanadium(V)-substituted tungstosulfate S_2VW_{17} isomers along with their characterization by X-ray structural analysis, IR, Raman, and ^{51}V NMR spectroscopies, and voltammetry. The one-electron-reduced $[S_2V^{IV}W_{17}O_{62}]^{6-}$ forms also have been prepared by bulk electrolysis and characterized by voltammetry and EPR spectroscopy

EXPERIMENTAL SECTION

Reagents. Unless otherwise stated, reagents were of analytical grade and used as received from WAKO. Tetrabutylammonium hexafluorophosphate (TCI), $n\text{-}Bu_4NPF_6$, recrystallized at least twice from ethanol, was used as the supporting electrolyte in all electrochemical measurements. Acetonitrile (LC–MS grade) was purchased from WAKO. A stock solution of V^V was prepared by dissolving 29.2 g of NH_4VO_3 (WAKO) and 20.0 g of NaOH (WAKO) in 500 mL of water.

Synthesis of 1-Vanadium-Substituted Tungstosulfate, 1-$[S_2VW_{17}O_{62}]^{5-}$ (1-S_2VW_{17}). $Na_2WO_4{\cdot}2H_2O$ (3.3 g) was dissolved in 97.8 mL of water followed by addition of 80 mL of acetonitrile. Concentrated H_2SO_4 (22.2 mL) was then carefully added in small aliquots with vigorous stirring. Next, the mixture was heated in a sealed bottle at 70 °C for 2 weeks to form $[S_2W_{18}O_{62}]^{4-}$. After cooling, 0.6 mL of the V^V stock solution was added, and this reaction mixture was refluxed for 3 days, during which time a tungsten unit of $[S_2W_{18}O_{62}]^{4-}$ became substituted with a vanadium one to form 1-$[S_2VW_{17}O_{62}]^{4-}$ as the major species. Any precipitate that formed was separated out after cooling. CH_3CN (60 mL) was then added to the now orange–yellow solution. After shaking and standing at room temperature for ca. 10 min, separation into two phases occurred. The colorless phase was discarded, and $n\text{-}Bu_4NBr$ was added to the orange–yellow phase. A yellow precipitate was collected by filtering, washed with water and ethanol, recrystallized from CH_3CN, and dried in vacuo (yield, 4.3 g). Anal. Calcd for $(n\text{-}Bu_4N)_5[1\text{-}SV_2W_{17}O_{62}]$: W, 57.4; V, 0.94; S, 1.18; C, 17.65; H, 3.33; N, 1.29. Found: W, 58.1; V, 1.03; S, 1.15; C, 17.37; H, 3.38; N, 1.28.

Synthesis of 4-Vanadium-Substituted Tungstosulfate, 4-$[S_2VW_{17}O_{62}]^{5-}$ (4-S_2VW_{17}). The only major difference in the synthesis of 1-S_2VW_{17} and 4-S_2VW_{17} is that in the latter case the addition of the V^V stock solution occurred at an earlier stage in the preparation. Thus, again, 3.3 g of $Na_2WO_4{\cdot}2H_2O$ was dissolved in 97.8 mL of water. However, to synthesize 4-S_2VW_{17}, this step was followed by addition of 0.6 mL of the V^V stock solution and 80 mL of acetonitrile. Next, 22.2 mL of concentrated H_2SO_4 was carefully added in small aliquots with vigorous stirring, and the mixture was heated in a sealed bottle at 80 °C for 3 days. Any precipitate that appeared during heating was again separated after cooling. Using this order of mixing reagents, 4-$[S_2VW_{17}O_{62}]^{5-}$, rather than 1-$[S_2VW_{17}O_{62}]^{5-}$, is the major species present in the orange–yellow solution. After 60 mL of CH_3CN was added, the solution was shaken and allowed to stand at room temperature for ca. 10 min, at which time separation into two phases occurred. The colorless phase was discarded, and $n\text{-}Bu_4NBr$ was added to the orange–yellow phase. The yellow precipitate (of a different shade than for 1-$SVW_{17}O_{62}$) was filtered off, washed with water and ethanol, recrystallized from CH_3CN, and dried in vacuo (yield, 4.3 g). Anal. Calcd for $(n\text{-}Bu_4N)_5[4\text{-}SVW_{17}O_{62}]$: W, 57.4; V, 0.94; S, 1.18; C, 17.65; H, 3.33; N, 1.29. Found: W, 57.2; V, 0.97; S, 1.17; C, 17.63; H, 3.43; N, 1.29.

Unfortunately, an isomerically pure bulk sample of 4-S_2VW_{17}, totally devoid of 1-S_2VW_{17}, could not be obtained (see spectroscopic evidence below) despite numerous attempts to optimize the preparative conditions and the use of a wide range of organic solvents for recrystallization. However, hand selection of a single crystal of pure 4-S_2VW_{17} enabled X-ray structural analysis to be achieved. The small difference in color (yellow for 1-S_2VW_{17} and orange–yellow for 4-S_2VW_{17}; Supporting Information, Figure S1) facilitated the distinction. Spectroscopic data confirmed that greater than 90% of the bulk solid was 4-$[S_2VW_{17}O_{62}]^{4-}$. A small amount of isomerization of 4-S_2VW_{17} probably always occurs during recrystallization in the same way that 4-$[P_2W_{17}O_{61}]^{10-}$ isomerizes in aqueous media to give 1-$[P_2W_{17}O_{62}]^{10-}$.[12]

$(n\text{-}Bu_4N)_4[S_2W_{18}O_{62}]$ as the symmetrical alpha isomer (α-S_2W_{18}) was prepared as described in the literature.[16d] The γ- form of S_2W_{18} also is known,[17l] but because only the symmetrical α structural form is found for 1- and 4-S_2VW_{17}, data comparisons were only made with α-S_2W_{18}

X-ray Crystallography of 1- and 4-S_2VW_{17}. X-ray single-crystal crystallographic data were collected with a Rigaku VariMax RAPID diffractometer using Mo Kα radiation. The structure was solved by direct methods[22] and expanded using Fourier techniques. Some of the non-hydrogen atoms were refined anisotropically. Hydrogen atoms were refined using the riding model. The final cycle of full-matrix least-squares refinement[23] on F^2 was based on 15 998 and 26 429 observed reflections and 810 and 1363 variable parameters for 1- and 4-S_2VW_{17}, respectively, and converged (largest parameter shift was 0.01 times its esd) with unweighted and weighted agreement factors of

$$R_1 = \sum ||F_o| - |F_c|| / \sum |F_o| = 0.339 \text{ for 1-}S_2VW_{17} \text{ and } 0.0236 \text{ for 4-}S_2VW_{17}\ (I > 2.00\sigma(I))$$

$$wR_2 = [\sum(w(F_o^2 - F_c^2)^2)/\sum w(F_o^2)^2]^{1/2} = 0.0700 \text{ for 1-}S_2VW_{17} \text{ and } 0.0400 \text{ for 4-}S_2VW_{17}$$

The standard deviation with unit weighting[24] was 1.06 for 1-S_2VW_{17} and 1.22 for 4-S_2VW_{17}. The maximum and minimum peaks on the final difference Fourier map correspond to 2.52 and −2.11 $e^-/Å^3$ for 1-S_2VW_{17} and 1.84 and −0.91 $e^-/Å^3$ for 4-S_2VW_{17}, respectively. The absolute structure was deduced on the basis of a Flack parameter of 0.017(6), which was calculated using 12 210 Friedel pairs for 4-S_2VW_{17} only.[25]

Neutral atom scattering factors were taken from Cromer and Waber.[26] Anomalous dispersion effects were included in F_{calc};[27] the values for $\Delta f'$ and $\Delta f''$ as well as for the mass attenuation coefficients are those of Creagh and McAuley.[28] All calculations for the structures of salts of 1- and 4-S_2VW_{17} were performed using the CrystalStructure, ver. 4.0, crystallographic software package (Rigaku) except for refinement, which was performed using SHELXL-97.[22,29]

Other Measurements. Voltammetric experiments were carried out at 25 ± 1 °C (298.2 K) with BAS 50W or 100W electrochemical workstations (BioAnalytical Systems). A standard three-electrode electrochemical cell arrangement was employed with a glassy carbon macrodisk (surface area 0.071 cm^2) as the working electrode, a platinum wire as the counter electrode, and Ag/Ag^+ (0.01 M $AgNO_3$ in CH_3CN) as the reference electrode. Unless otherwise stated, the scan rate used in voltammetric experiments was 100 mV s^{-1}. Potentials measured versus Ag/Ag^+ was converted to the Fc/Fc^+ (Fc = ferrocene) scale by analysis of cyclic voltammetric data for oxidation in ferrocene in acetonitrile (0.1 M $n\text{-}Bu_4NPF_6$). Before each measurement, the glassy carbon electrode (GCE) was polished with an aqueous 0.1 μm diamond slurry and washed with distilled water. Bulk electrolysis experiments were undertaken with the same instrumentation and electrodes as used in voltammetry except that in this case a carbon fiber cloth with a large surface area was used as the working electrode and solutions containing the working, reference, and auxiliary electrodes were separated by salt bridges. The appropriate controlled potential was applied to generate the one-electron-reduced species. All solutions used in electrochemical experiments were purged with argon gas for at least 10 min to remove dissolved oxygen.

dx.doi.org/10.1021/ic402994q | Inorg. Chem. 2014, 53, 4891–4898

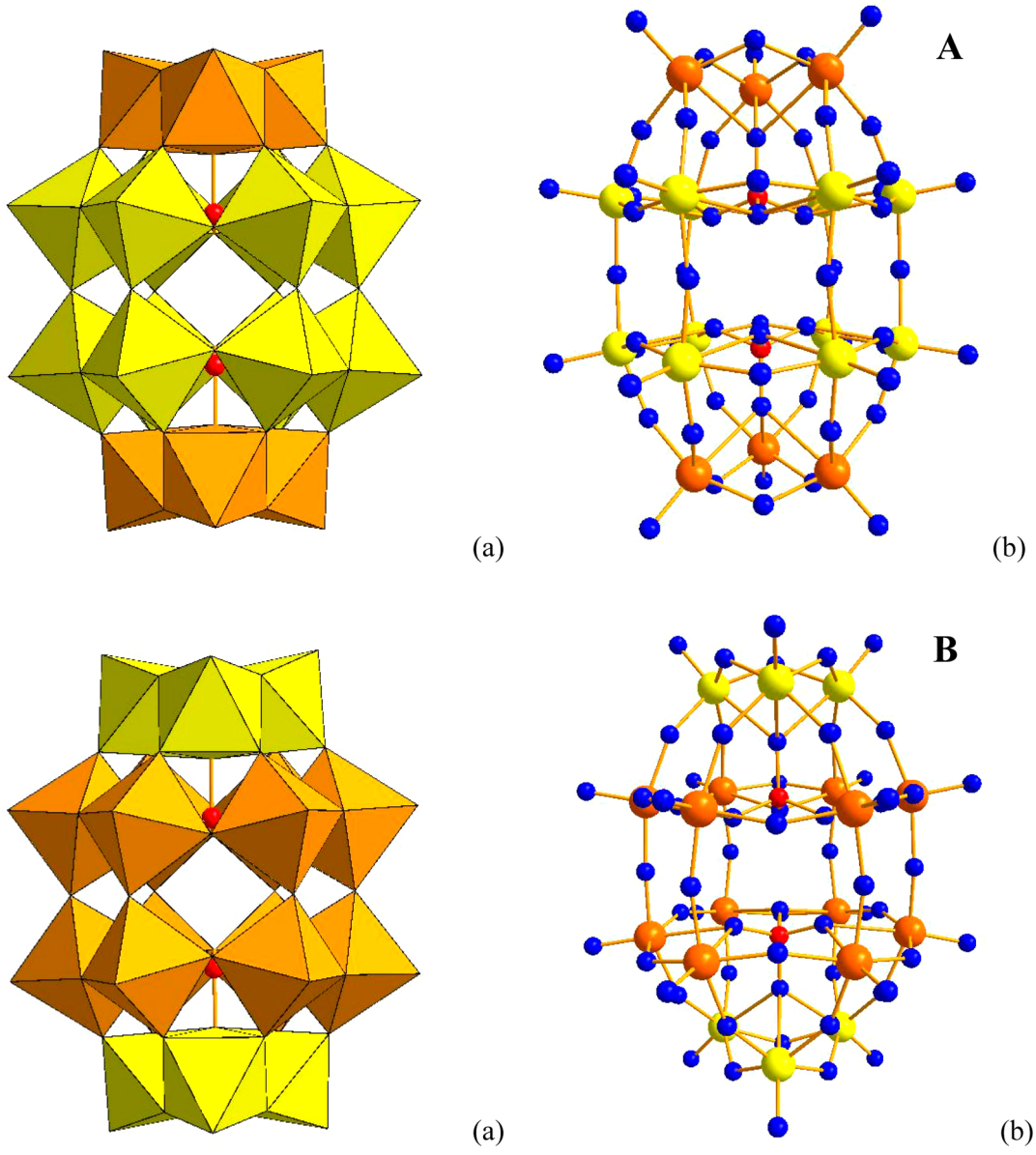

Figure 1. Polyhedral (a) and stick and ball (b) representations of structures for (A) 1-S_2VW_{17} and (B) 4-S_2VW_{17} obtained by X-ray crystallographic analysis. In panel b, yellow balls represent W only sites; orange, W or V; red, sulfur; and blue, oxygen.

^{51}V NMR spectra were obtained with a JEOL model JNM-LA400 spectrometer at 105.03 MHz. An inner tube containing D_2O was used as an instrumental lock. Vanadium chemical shifts were referenced to neat $VOCl_3$. For the EPR measurements, following bulk electrolysis under argon, the one-electron-reduced solution was transferred into an EPR tube and immediately frozen in liquid nitrogen to prevent aerial reoxidation. X-band (ca. 9.5 GHz) EPR spectra were recorded at 120 K with a Bruker ESP380E CW/FT spectrometer using the standard rectangular TE_{012} cavity in association with a Bruker VT 4111 temperature controller and nitrogen gas flow insert. Microwave frequencies were measured with an EIP microwave 548A frequency counter and the g factors were determined by reference to the F^+ resonance line in CaO with a g value of 2.0001 ± 0.001.[30] EPR spectrum simulations were performed using the Bruker SOPHE software suite.[31] Raman spectra were recorded at 20 °C on a Horiba Jobin Yvon model HR-800 instrument. The argon line at 514.5 nm was used for excitation. IR spectra were obtained by the KBr pellet method with a Jasco FT/IR-460 plus spectrophotometer. UV−vis spectra were recorded on a Jasco model V-670 spectrophotometer with a quartz cell having a path length of 1 mm.

Tungsten and vanadium elemental analysis in 1- and 4-S_2VW_{17} were carried out with a Shimadzu ICPE-9000 spectrometer after dissolving the sample in aqueous 0.1 M NaOH. The carbon, hydrogen, nitrogen, and sulfur content was obtained with a PerkinElmer CHNS/O 2400II analyzer.

RESULTS AND DISCUSSION

Structures of 1- and 4-S_2VW_{17}. Single-crystal X-ray structural analysis shows that both isomers have the α-Wells−Dawson configuration (Figure 1). Disorder is evident at vanadium locations in both structures, which is common in vanadium-substituted polyoxometalates.[32] However, in the case of 1-S_2VW_{17}, disorder is concentrated at the polar sites (Figure 1a), whereas in 4-S_2VW_{17}, disorder is prevalent at the belt sites (Figure 1b). The much higher occupancy of vanadium at the polar sites in the structure in Figure 1a leads to its assignment as the 1-S_2VW_{17} isomer, whereas the higher occupancy in the structure in Figure 1b at the belt sites leads to its 4-S_2VW_{17} isomer assignment.

dx.doi.org/10.1021/ic402994q | Inorg. Chem. 2014, 53, 4891−4898

Table 1. Crystal Data and Structure Refinement for 1-S_2VW_{17} and 4-S_2VW_{17}

	1-S_2VW_{17}	4-S_2VW_{17}
empirical formula	$C_{88}H_{192}N_9O_{62}S_2VW_{17}$	$C_{62}H_{143}N_6O_{62}S_2VW_{17}$
FW (g mol^{-1})	5609.02	5205.33
T (K)	123(1)	123(1)
radiation (λ, Å)	0.71075	0.71075
crystal system	monoclinic	orthorhombic
space group	$C2/c$ (15)	$P2_12_12_1$ (19)
a (Å)	26.1401(5)	18.3309(4)
b (Å)	15.5551(3)	20.3938(4)
c (Å)	35.844(3)	30.927(3)
β (deg)	105.853(8)	
V (Å^3)	14 020.26(135)	11 561.65(117)
Z	4	4
d_{calcd} g/cm^3	2.657	2.990
no. obs (all data)	15 998	26 429
GOF	1.063	1.221
final R indices ($I > 2.00\sigma(I)$)[a]	$R_1 = 0.0339$	$R_1 = 0.0236$
final R indices (all data)[b]	$R = 0.0455$	$R = 0.0246$
	$wR_2 = 0.0700$	$wR_2 = 0.0400$

[a] $R_1 = \sum ||F_o| - |F_c|| / \sum |F_o|$ ($I > 2.00\sigma(I)$). [b] $wR_2 = [\sum(w(F_o^2 - F_c^2)^2)/\sum w(F_o^2)^2]^{1/2}$.

Table 1 summarizes the crystallographic data for 1- and 4-S_2VW_{17}. The bond lengths and bond angles between the tungsten, vanadium, sulfur, and oxygen atoms for both isomers are listed in the Supporting Information, Tables S1−S4. The mean lengths of selected bonds are provided in Table 2 and are

Table 2. Selected Mean Bond Lengths (Å) for 1-S_2VW_{17}, 4-S_2VW_{17}, and S_2W_{18}[a]

		1-S_2VW_{17}	4-S_2VW_{17}	S_2W_{18}[b]
W−O_d	polar	1.69	1.70	1.76
W−O_d	belt	1.70	1.69	1.72
W−O_b		1.90	1.90	1.91
W−O_c		1.91	1.91	1.92
W−O_a		2.43	2.48	2.48
S−O_a		1.48	1.48	1.50

[a] O_a, oxygen bonded with sulfur atom; O_b, corner-shared oxygen; O_c, edge-shared oxygen; and O_d, terminal oxygen. [b] Calculated from the data in ref 16d.

compared therein with those of S_2W_{18}.[16d] All of the mean bond lengths of S_2VW_{17} are similar to those for S_2W_{18}. However, a characteristic feature of the structure is that the mean bond lengths between tungsten, vanadium, and terminal oxygens are shorter than in the parent S_2W_{18}. A summary of the overall dimensions for 1- and 4-S_2VW_{17} and S_2W_{18} is provided in the Supporting Information, Figure S2. For all three polyoxometalates, the six metal atoms in the belt positions and the sulfur atom are located in almost the same plane, with slightly larger deviations for 4-S_2VW_{17} and S_2W_{18}. In addition, each of the six metal atoms in the belt positions is located at the apex of a regular hexagon with a bond angle of 120 ± 0.5° between three adjacent metal atoms, whereas each of the three metal atoms at the polar positions is located at the apex of regular triangle with a bond angle between them of 60 ± 0.5°. The two sulfur atoms and two oxygen atoms bonded to the metal atoms at the polar positions are located in a straight line for all three polyoxometalates. Mean bond angles around vanadium atoms are summarized in Table 3.

Table 3. Mean Bond Angles (Degrees) around Vanadium Atoms in 1-S_2VW_{17} and 4-S_2VW_{17}[a]

	1-S_2VW_{17}	4-S_2VW_{17}
O_d−V−O_{wd}	103.29	99.45
O_d−V−O_{vs}	102.14	102.96
O_d−V−O_{vd}		99.87
O_d−V−O_a	172.57	172.65
O_{vs}−V−O_{vs}	86.67	153.91
O_{wd}−V−O_{wd}	85.31	
O_{vs}−V−O_{wd} cis	88.45	86.67
O_{vs}−V−O_{wd} trans	154.54	
O_{vd}−V−-O_{wd}		160.49
O_{vs}−V−O_{vd}		88.91
O_a−V−O_{wd}	82.04	80.98
O_a−V−O_{vs}	72.66	77.03
O_a−V−O_{vd}		80.18

[a] O_a, oxygen bonded with a sulfur atom; O_d, terminal oxygen; O_{vs}, oxygen bonded with a vanadium atom in the same plane; O_{vd}, oxygen bonded with vanadium atom in a different plane; and O_{wd}, oxygen bonded with a tungsten atom in a different plane.

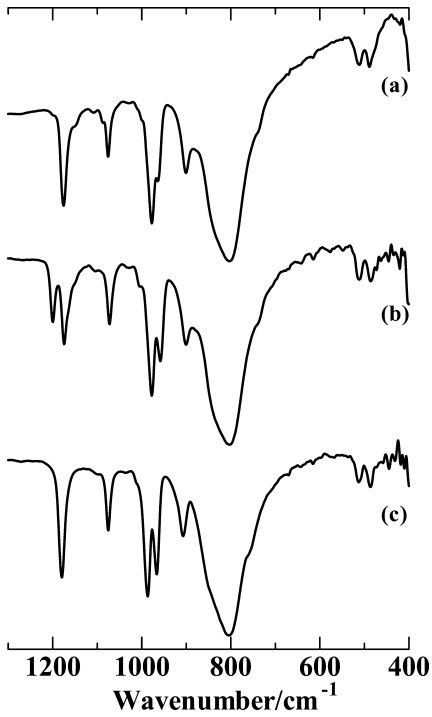

Figure 2. IR spectra of KBr pellets for n-Bu_4N^+ salts of (a) 1-S_2VW_{17}, (b) 4-S_2VW_{17}, and (c) S_2W_{18}.

IR and Raman Spectroscopy of 1- and 4-S_2VW_{17}. Figure 2 shows the IR spectra of the n-Bu_4N^+ salts of 1- and 4-S_2VW_{17} and S_2W_{18}. The positions of selected IR and Raman bands (Supporting Information, Figure S3) and assignments are summarized in Table 4.[33] The overall pattern of the IR spectra for 1- and 4-S_2VW_{17} is the same as that for α-S_2W_{18}. As expected, the 1- and 4-S_2VW_{17} anions have a Wells−Dawson structure that is associated with the symmetries of α-S_2W_{18}, consistent with the X-ray crystallographic results. The IR band found at ca. 1180 cm^{-1} for S_2W_{18} and ascribed to the S−O bond is split into two bands at 1201 and 1174 cm^{-1} for 4-S_2VW_{17}, but it is detected as a single band for 1-$S_2V_2W_{16}$ at 1177 cm^{-1}. The same IR band splitting behavior was also observed at IR peaks for the P−O

dx.doi.org/10.1021/ic402994q | Inorg. Chem. 2014, 53, 4891−4898

Table 4. Vibrational Frequencies (cm^{-1}) for 1-S_2VW_{17}, 4-S_2VW_{17}, and S_2W_{18}[a]

compound	ν_{IR}(W−O_d)	ν_{IR}(W−O_b−W)	ν_{IR}(W−O_c−W)	ν_{IR}(S−O_a)	ν_{Raman}(W−O_d)
1-S_2VW_{17}	980, 965(sh)	901	804	1177, 1077	997
4-S_2VW_{17}	977, 959	901	804	1201, 1174, 1073	997
S_2W_{18}	986, 966[b)]	906[b]	804[b]	1180, 1076[b]	1001 (1007)[b,c]

[a]O_a, oxygen bonded with a sulfur atom; O_b, octahedral corner-sharing oxygen; O_c, octahedral edge-sharing oxygen; and O_d, terminal oxygen. [b]Data from ref 12d. [c]Dissolved in CH_3CN.

stretching region of 1-P_2VW_{17} and 4-P_2VW_{17}.[34] However, no IR peak splitting was observed in the case of the IR spectra for 1-P_2FeW_{17} and 4-P_2FeW_{17}.[35] IR peak splitting would be generated from a difference in the symmetry of the S−O and P−O bonds. Unfortunately, no reasonable theoretical reasons are available to explain this IR splitting behavior. Unfortunately, there are currently few samples of metal-substituted tungstosulfates. This issue may be solved in the future if many other metal-substituted tungstosulfates are prepared and characterized. The other IR band attributed to the S−O bond was detected at ca. 1075 cm^{-1} for all three polyoxometalates. In S_2W_{18}, the IR band at 1180 cm^{-1} is ascribed to the asymmetric stretching mode between sulfur and oxygen attached to a tungsten ion in a belt position, whereas that at 1076 cm^{-1} is attributed to the asymmetric stretching mode between sulfur and oxygen attached to tungsten in a polar position for 1- S_2VW_{17} and 4- S_2VW_{17}. The IR bands at ca. 980 and 960 cm^{-1} for S_2W_{18} are shifted to a slightly lower wavenumber for 1- and 4-S_2VW_{17}. The relative intensity of the band at ca. 900 cm^{-1} in 1- and 4-S_2V_{17} decreases relative to that in S_2W_{18}. Additionally, the Raman band associated with the symmetric stretching vibration of W−O (terminal) is shifted to lower wavenumbers when vanadate replaces tungstate. An analogous situation applies in the IR spectra of $XV_xW_{12-x}O_{40}^{(3+x)-}$ (X = P, As; x = 0−2) polyoxometalates when tungsten is substituted by vanadium.[19b]

UV−Vis Spectra. Figure 3 shows UV−vis spectra of 1- and 4-S_2VW_{17} and S_2W_{18} in acetonitrile. The absorbance at ca. 250

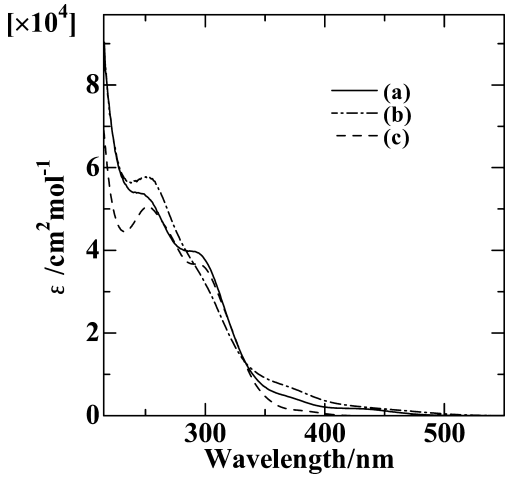

Figure 3. UV−vis spectra of (a) 1-S_2VW_{17}, (b) 4-S_2VW_{17}, and (c) S_2W_{18} in acetonitrile.

and 370 nm increases and that at ca. 295 nm decreases when vanadium is introduced. The molar absorption coefficients at 253 nm are 5.05, 5.51, and 5.73 (× 10^4 cm^2 mol^{-1}) for 1-S_2VW_{17}, 4-S_2VW_{17}, and S_2W_{18}, respectively. The absorption at ca. 260 nm is attributed to the LMCT (O → W) band.[36] It has been suggested that the broad band at around 370 nm, observed with 1- and 4-S_2VW_{17} but not for S_2W_{18}, can be attributed to an O → V LMCT band.

NMR Spectroscopy of 1- and 4-S_2VW_{17}. ^{51}V NMR spectra in CH_3CN show one sharp resonance at 560 ppm for 1-S_2VW_{17}, whereas for 4-S_2VW_{17}, the sharp resonance at 572 ppm is accompanied by a minor one at 561 ppm, indicating that a small amount (≤5%) of 1-S_2VW_{17} is present (Supporting Information, Figure S4). No fully isomerically pure sample of bulk 4-S_2VW_{17} could be prepared, although a hand-picked isomerically pure single crystal suitable for X-ray structural analysis was obtained (see Experimental Section).

EPR Spectra of Reduced 1- and 4-S_2VW_{17}. The EPR spectra of MeCN solutions of 1- and 4-S_2VW_{17} (0.5 mM) electrochemically reduced by one electron (see later) and then frozen at 120 K exhibited strong resonances because of V^{IV} in sites of orthorhombic symmetry. The spin Hamiltonian parameters of the V^{IV} ion in the most prominent sites are listed in Table 5, and the experimental and simulated spectra are compared in Figures 4 and 5 for 1- and 4-S_2VW_{17}, respectively. The EPR spectrum of reduced 4-S_2VW_{17} shows the presence of a small amount of reduced 1-S_2VW_{17} as well as about 10% of another species having a very similar EPR spectrum as that of 4-S_2VW_{17}. The latter may be attributed to a small amount of protonated species, as is encountered in some of the one-electron-reduced Keggin polyoxometalates that have been described previously.[32,37] As can be seen from the data in Table 5, the spin Hamiltonian parameters for reduced 1-S_2VW_{17} are similar to those found for the reduced Keggin polyoxometalates XVW_{11} (X = P, As).[32,37] However, the value of g_z for reduced 4-S_2VW_{17} is significantly different, indicating that, in this case, the V^{IV} ion is in a different site compared to that of both reduced 1-S_2VW_{17} and the Keggin complexes. This is consistent with the notion that the vanadium resides in a polar site in reduced 1-S_2VW_{17} and a belt site in reduced 4-S_2VW_{17} (Table 3). Thus, the EPR spectra of the one-electron-reduced forms of the two isomers are consistent with structures deduced from the X-ray analysis of the nonreduced isolated solids, implying that no major structural change occurs on reduction. A comparison of the fractional spin densities in the d_{xy} orbitals, calculated using the expressions in ref 38 and listed in Table 5, shows that the unpaired electron is more delocalized when the V^{IV} ion is in a belt rather than a polar site. This may be reflected in the enhanced reactivity of the 4-S_2VW_{17} isomer.

Voltammetric Behavior of 1- and 4-S_2VW_{17}. A comparison of the very rich cyclic voltammetric behavior of 1- and 4-S_2VW_{17} (four well-defined processes) and S_2W_{18} (six well-defined processes) in CH_3CN containing 0.1 M n-Bu_4NPF_6 as the supporting electrolyte is shown in Figure 6. Reversible potentials calculated from the average of the reduction and oxidation peak potentials are summarized in Table 6. All processes are diffusion-controlled. A diffusion coefficient of 5.49 × 10^{-6} cm^2 s^{-1} for 1-S_2VW_{17} was found from the analysis of the peak current for reduction (I_p) as a function of the scan rate over

dx.doi.org/10.1021/ic402994q | Inorg. Chem. 2014, 53, 4891−4898

Table 5. Spin Hamiltonian Parameters for 1-S_2VW_{17}, 4-S_2VW_{17}, and Related Species[a]

compound	g_x	g_y	g_z	A_x	A_y	A_z	P	β^2	ref
1-S_2VW_{17}	1.969	1.967	1.919	60.5	55.5	166.5	0.30	0.91	this study
4-S_2VW_{17}	1.963	1.957	1.882	55.0	57.5	163.5	0.30	0.85	this study
PVW_{11}	1.969	1.971	1.914	56.5	61.5	169.5	0.4	0.92	37
$AsVW_{11}$	1.970	1.973	1.914	57.0	60.0	168.5	0.3	0.91	37
SVW_{11}	1.969	1.971	1.908	59.0	62.5	171.0	0.35	0.92	32

[a]The units for P (the ^{51}V quadrupole interaction) and the components of A (the ^{51}V hyperfine interaction) are $\times 10^{-4}$ cm^{-1}. β^2 is the fractional spin density in the d_{xy} orbital. Uncertainties for g values are ± 0.001, for A values are $\pm 0.5 \times 10^{-4}$ cm^{-1}, and for P values are $\pm 0.02 \times 10^{-4}$ cm^{-1}.

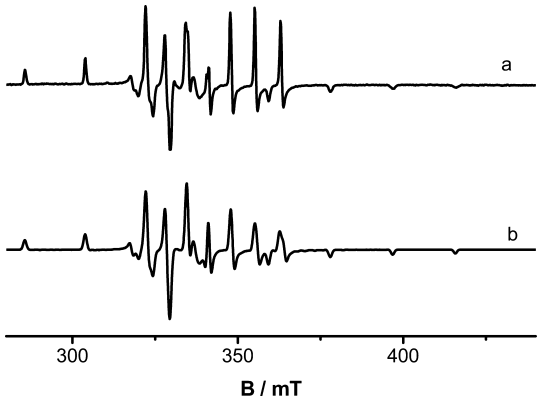

Figure 4. (a) EPR spectrum in acetonitrile containing 0.1 M *n*-Bu_4NPF_6 after one-electron reduction of 0.5 mM 1-S_2VW_{17} and freezing at 120 K. Spectrometer settings are as follows: microwave frequency, 9.426 GHz; microwave power, 4.18 mW; receiver gain, 1.0×10^5; 100 kHz modulation amplitude, 0.25 mT; field scan range/time, 160 mT/84 s; and recorder time constant, 82 ms. (b) Simulated spectrum using the spin Hamiltonian parameters listed in Table 5 and a Gaussian line shape with a width of 5×10^{-4} cm^{-1}.

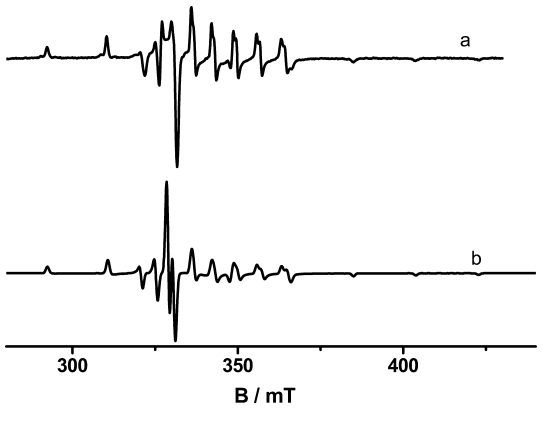

Figure 5. (a) EPR spectrum in acetonitrile (0.1 M *n*-Bu_4NPF_6) after one-electron reduction of 0.5 mM 4-S_2VW_{17} and freezing at 120 K. Spectrometer settings are as follows: microwave frequency, 9.432 GHz; microwave power, 5.26 mW; receiver gain, 5.0×10^4; 100 kHz modulation amplitude, 0.20 mT; field scan range/time, 160 mT/82 s; and recorder time constant, 82 ms. (b) Simulated spectrum using the spin Hamiltonian parameters listed in Table 5 and a Gaussian line shape with a width of 5×10^{-4} cm^{-1}.

the range of 20−500 mV s^{-1} and from use of the Randles−Sevcik relationship (eq 1)

$$I_p = (2.69 \times 10^5) n^{3/2} A D_0^{1/2} C_0 \nu^{1/2} \quad (1)$$

where $n = 1.0$ is the number of electrons transferred, A is the surface area of the electrode, D is the diffusion coefficient, C_0 is

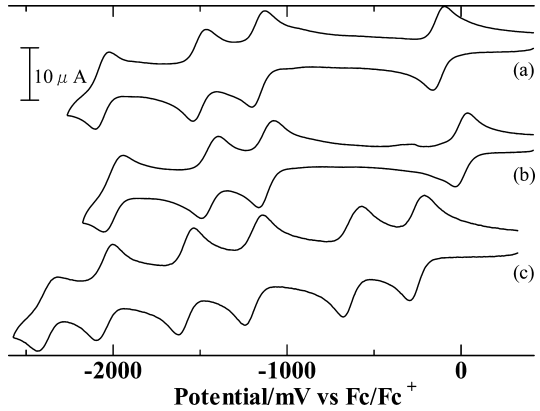

Figure 6. Cyclic voltammograms obtained at 25 °C with a glassy carbon electrode using a scan rate of 100 mV s^{-1} for 0.5 mM (a) 1-S_2VW_{17}, (b) 4-S_2VW_{17}, and (c) S_2W_{18} in acetonitrile (0.1 M *n*-Bu_4NPF_6).

the concentration of the sample, and ν is the scan rate. The D_0 value for 4-S_2VW_{17} could not be determined precisely because of uncertainty in the purity of this isomer. However, the value should be very similar as that of 1-S_2VW_{17} (same molecular weight). Coulometric analysis of data obtained under conditions of exhaustive bulk electrolysis confirmed that a one-electron charge transfer is associated with this V^V/V^{IV} reduction process. The peak-to-peak (ΔE_p) separation between the reduction and oxidation peaks ranged from 70 to 100 mV, as expected for reversible or close to reversible processes after allowing for a small level of uncompensated resistance (the known reversible $Fc^{0/+}$ process gave similar ΔE_p values). The EPR spectra after exhaustive reductive bulk electrolysis of 1- and 4-S_2VW_{17} at a constant potential slightly more negative than the reversible potential for the first reduction process exhibited only the typical V (IV) resonances as assigned above. Thus, the first reduction process should be ascribed to the reduction of vanadium V to IV for both 1- and 4-S_2VW_{17} (eq 2).

$$[S_2V^VW_{17}]^{5-} + e^- = [S_2V^{IV}W_{17}]^{6-} \quad (2)$$

The reduction of vanadium in other Keggin- and Wells−Dawson-type vanadium-substituted polyoxometalates occurs at more positive potentials than for reduction of tungsten in the polyoxometalate framework of the parent polyoxometalate.[32,37,39] Similarly, for both 1- and 4-S_2VW_{17}, it was found that the reduction of vanadium occurs at a more positive potential than reduction of W(VI) in the framework of S_2W_{18}. In addition, the first reduction process for 4-S_2VW_{17} occurs at a more positive potential than for 1-S_2VW_{17}, which is analogous to the observation that the first reduction process for 4-P_2VW_{17} occurs at a more positive value than that found for 1-P_2VW_{17}.[34] In terms of the Wells−Dawson class of polyoxometalates, a vanadium atom in a belt site should be more easily reduced than

dx.doi.org/10.1021/ic402994q | Inorg. Chem. 2014, 53, 4891−4898

Table 6. Midpoint Potentials[a,b] (E_{mid}/mV vs Fc/Fc$^+$) for Reduction of $[S_2V_xW_{18-x}O_{62}]^{(4+x)-}$ (x = 0, 1)

	redox process[c]						
compounds	$V^V \rightarrow V^{IV}$	0W → IW	IW → IIW	IIW → IIIW	IIIW → IVW	IVW → VW	VW → VIW
1-S_2VW_{17}	−130	−1170	−1500	−2000			
4-S_2VW_{17}	0	−1120	−1450	−2000			
S_2W_{18}		−260	−640	−1200	−1580	−2050	−2380

[a] $E_{mid} = (E_p^{red} + E_p^{ox})/2$, where E_p^{red} and E_p^{ox} are the reduction and oxidation peak potentials, respectively. [b] Measured in CH_3CN containing 0.1 M n-Bu_4NPF_6 as the supporting electrolyte. [c] 0, I, II, III, IV, V, and VI indicate the number of tungstens reduced.

one in a polar site;[40] hence, belt-sited vanadium-substituted polyoxometalates, 4-X_2VW_{17}, should be superior oxidative catalysts to polar-sited vanadium-substituted polyoxometalates, 1-X_2VW_{17}. The 4-X_2VW_{17} isomers, in all cases to date, seem to be more reactive than 1-X_2VW_{17} in both the V^V and V^{IV} forms.

CONCLUSIONS

Two new vanadium-substituted tungstosulfates, 1- and 4-S_2VW_{17}, were prepared and isolated as tetrabutyl ammonium salts from an aqueous−organic solvent mixture. 1-S_2VW_{17} could be isolated in pure form but not 4-S_2VW_{17}, where the 1-S_2VW_{17} isomer, spontaneously generated from recrystallization, is always present in the bulk n-Bu_4N^+ salt of 4-S_2VW_{17}. The selective preparation of 1- and 4-S_2VW_{17} was achieved by altering the order of addition of the reagents in the preparation procedure. Both polyoxometalates were characterized by elemental analysis, X-ray crystallography, ^{51}V NMR, IR, Raman, and UV−vis spectroscopies, and voltammetry. The one-electron 1- and 4-S_2VW_{17} reduced forms were characterized by EPR spectroscopy and voltammetry. X-ray crystallographic analysis showed that both isomers have the symmetrical α Wells−Dawson-type structure, where the substituted vanadium is located at a polar site in 1-S_2VW_{17} and at a belt site in 4-S_2VW_{17}. In 1- and 4-S_2VW_{17}, the bond lengths between the metal atoms and terminal oxygen of 1- and 4-S_2VW_{17} are shorter than those in S_2W_{18}. Four essentially reversible reduction processes were observed for 1- and 4-S_2VW_{17} under conditions used for cyclic voltammetry (CH_3CN containing 0.1 M n-Bu_4NPF_6 as the supporting electrolyte). Analysis of the EPR spectra after one-electron bulk electrolysis showed that the first process is a result of the reduction of the V^V to the V^{IV} redox state. In addition, $V^{V/IV}$ reduction of 4-S_2VW_{17} is more easily achieved than for 1-S_2VW_{17}.

ASSOCIATED CONTENT

Supporting Information

Dimension comparisons of 1-S_2VW_{17}, 4-S_2VW_{17}, and S_2W_{18}; bond lengths and bond angles of 1-S_2VW_{17} and 4-S_2VW_{17} derived from X-ray crystallography; and Raman and ^{51}V NMR spectra of 1-S_2VW_{17} and 4-S_2VW_{17}. This material is available free of charge via the Internet at http://pubs.acs.org.

AUTHOR INFORMATION

Corresponding Author

*E-mail: chuji@kochi-u.ac.jp.

Author Contributions

The manuscript was written through contributions of all authors. All authors have given approval to the final version of the manuscript.

Notes

The authors declare no competing financial interest.

ACKNOWLEDGMENTS

This work was supported by a Grant-in-Aid for Scientific Research (no. 25410095) from the Ministry of Education, Culture, Sports, Science and Technology of Japan, a Kochi University President's Discretionary Grant provided by Kochi University, and the Australian Research Council.

REFERENCES

(1) Pope, M. T. *Heteropoly and Isopoly Oxometalates*; Springer: Berlin, Germany, 1983.

(2) *Polyoxometalate Chemistry: From Topology via Self-Assembly to Applications*; Pope, M. T., Müller, A., Eds.; Kluwer Academic Publishers: Boston, MA, 2001.

(3) *Polyoxometalate Chemistry for Nano-Composite Design*; Yamase, T., Pope, M. T., Eds.; Kluwer Academic/Plenum Publishers: New York, 2002.

(4) *Polyoxometalate Molecular Science*; Borrás-Almenar, J. J., Coronado, E., Müller, A., Pope, M. T., Eds.; Kluwer Academic Publishers: Boston, MA, 2003.

(5) Ueda, T.; Kotsuki, H. *Heterocycle* **2008**, *76*, 73−97.

(6) Carraro, M.; Sartorel, A.; Scorrano, G.; Carofiglio, T.; Bonchio, M. *Synthesis* **2008**, 1971−1978.

(7) Hill, C. L. *J. Mol. Catal. A: Chem.* **2007**, *262*, 2−6.

(8) Neumann, R.; Khenkin, A. M. *Chem. Commun.* **2006**, 2529−2538.

(9) Mizuno, N.; Yamaguchi, K. *Chem. Rec.* **2006**, *6*, 12−22.

(10) Kozhevnikov, I. V. *Chem. Rev.* **1998**, *98*, 171−198.

(11) Mizuno, N.; Misono, M. *Chem. Rev.* **1998**, *98*, 199−217.

(12) Klemperer, W. G. *Inorg. Synth.* **1990**, *27*, 71−135.

(13) (a) Mialane, P.; Dolbecq, A.; Secheresse, F. *Chem. Commun.* **2006**, 3477−3485. (b) Zheng, S.-T.; Yang, G.-Y. *Chem. Soc. Rev.* **2012**, *41*, 7623−7646.

(14) (a) Li, H.; She, Y.; Wang, T. *Front. Chem. Sci. Eng.* **2012**, *6*, 356−368. (b) Shaik, S.; Hirao, H.; Kumar, D. *Acc. Chem. Res.* **2007**, *40*, 532−542.

(15) (a) Himeno, S.; Saito, A.; Hori, T. *Bull. Chem. Soc. Jpn.* **1990**, *63*, 1602−1606. (b) Maeda, K.; Himeno, S.; Saito, A.; Hori, T. *Bull. Chem. Soc. Jpn.* **1993**, *66*, 1693−1698. (c) Ueda, T.; Sano, K.-I.; Himeno, S.; Hori, T. *Bull. Chem. Soc. Jpn.* **1997**, *70*, 1093−1099. (d) Himeno, S.; Sano, K.; Niiya, H.; Yamazaki, Y.; Ueda, T.; Hori, T. *Inorg. Chim. Acta* **1998**, *281*, 214−220. (e) Long, D.-L.; Koegerler, P.; Cronin, L. *Angew. Chem., Int. Ed.* **2004**, *43*, 1817−1820. (f) Yan, J.; Long, D.-L.; Cronin, L. *Angew. Chem., Int. Ed.* **2010**, *49*, 4117−4120. (g) Corella-Ochoa, M. N.; Miras, H. N.; Kidd, A.; Long, D.-L.; Cronin, L. *Chem. Commun.* **2011**, *47*, 8799−8801. (h) Long, D.-L.; Yan, J.; Ruiz de la Oliva, A.; Busche, C.; Miras, H. N.; Errington, R. J.; Cronin, L. *Chem. Commun.* **2013**, *49*, 9731−9733.

(16) (a) Himeno, S.; Hori, T.; Saito, A. *Bull. Chem. Soc. Jpn.* **1989**, *62*, 2184−2188. (b) Hori, T.; Tamada, O.; Himeno, S. *J. Chem. Soc., Dalton Trans.* **1989**, 1491−1497. (c) Himeno, S.; Osakai, T.; Saito, A.; Maeda, K.; Hori, T. *J. Electroanal. Chem.* **1992**, *337*, 371−374. (d) Himeno, S.; Tatewaki, H.; Hashimoto, M. *Bull. Chem. Soc. Jpn.* **2001**, *74*, 1623−1628.

(17) (a) Cooper, J. B.; Way, D. M.; Bond, A. M.; Wedd, A. G. *Inorg. Chem.* **1993**, *32*, 2416−2420. (b) Bond, A. M.; Cooper, J. B.; Marken, F.; Way, D. M. *J. Electroanal. Chem.* **1995**, *396*, 407−418. (c) Bond, A. M.; Way, D. M.; Wedd, A. G.; Compton, R. G.; Booth, J.; Eklund, J. C. *Inorg. Chem.* **1995**, *34*, 3378−3384. (d) Way, D. M.; Bond, A. M.; Wedd, A. G. *Inorg. Chem.* **1997**, *36*, 2826−2833. (e) Way, D. M.; Cooper, J. B.; Sadek,

M.; Vu, T.; Mahon, P. J.; Bond, A. M.; Brownlee, R. T. C.; Wedd, A. G. *Inorg. Chem.* **1997**, *36*, 4227−4233. (f) Bond, A. M.; Eklund, J. C.; Tedesco, V.; Vu, T.; Wedd, A. G. *Inorg. Chem.* **1998**, *37*, 2366−2372. (g) Way, D. M.; Cooper, J. B.; Sadek, M.; Vu, T.; Mahon, P. J.; Bond, A. M.; Brownlee, R. T. C.; Wedd, A. G. *Inorg. Chem.* **1998**, *37*, 604−604. (h) Eklund, J. C.; Bond, A. M.; Humphrey, D. G.; Lazarev, G.; Vu, T.; Wedd, A. G.; Wolfbauer, G. *J. Chem. Soc., Dalton Trans.* **1999**, 4373−4378. (i) Bond, A. M.; Vu, T.; Wedd, A. G. *J. Electroanal. Chem.* **2000**, *494*, 96−104. (j) Bond, A. M.; Coomber, D. C.; Feldberg, S. W.; Oldham, K. B.; Vu, T. *Anal. Chem.* **2001**, *73*, 352−359. (k) Hultgren, V. M.; Bond, A. M.; Wedd, A. G. *J. Chem. Soc., Dalton Trans.* **2001**, 1076−1082. (l) Richardt, P. J. S.; Gable, R. W.; Bond, A. M.; Wedd, A. G. *Inorg. Chem.* **2001**, *40*, 703−709. (m) Richardt, P. J. S.; White, J. M.; Tregloan, P. A.; Bond, A. M.; Wedd, A. G. *Can. J. Chem.* **2001**, *79*, 613−620. (n) Juraja, S.; Vu, T.; Richardt, P. J. S.; Bond, A. M.; Cardwell, T. J.; Cashion, J. D.; Fallon, G. D.; Lazarev, G.; Moubaraki, B.; Murray, K. S.; Wedd, A. G. *Inorg. Chem.* **2002**, *41*, 1072−1078. (o) Ruther, T.; Jackson, W. R.; Bond, A. M. *Aust. J. Chem.* **2002**, *55*, 691−694. (p) Keyes, T. E.; Gicquel, E.; Guerin, L.; Forster, R. J.; Hultgren, V.; Bond, A. M.; Wedd, A. G. *Inorg. Chem.* **2003**, *42*, 7897−7905. (q) Ruether, T.; Hultgren, V. M.; Timko, B. P.; Bond, A. M.; Jackson, W. R.; Wedd, A. G. *J. Am. Chem. Soc.* **2003**, *125*, 10133−10143. (r) Seery, M. K.; Guerin, L.; Forster, R. J.; Gicquel, E.; Hultgren, V.; Bond, A. M.; Wedd, A. G.; Keyes, T. E. *J. Phys. Chem. A* **2004**, *108*, 7399−7405. (s) Zhang, J.; Bond, A. M.; Richardt, P. J. S.; Wedd, A. G. *Inorg. Chem.* **2004**, *43*, 8263−8271. (t) Zhang, J.; Bhatt, A. I.; Bond, A. M.; Wedd, A. G.; Scott, J. L.; Strauss, C. R. *Electrochem. Commun.* **2005**, *7*, 1283−1290. (u) Zhang, J.; Bond, A. M.; MacFarlane, D. R.; Forsyth, S. A.; Pringle, J. M.; Mariotti, A. W. A.; Glowinski, A. F.; Wedd, A. G. *Inorg. Chem.* **2005**, *44*, 5123−5132. (v) Mariotti, A. W. A.; Xie, J.; Abrahams, B. F.; Bond, A. M.; Wedd, A. G. *Inorg. Chem.* **2007**, *46*, 2530−2540. (w) Bond, A. M.; Eklund, J. C.; Fay, N.; Richardt, P. J. S.; Wedd, A. G. *Inorg. Chim. Acta* **2008**, *361*, 1779−1783.

(18) (a) Himeno, S.; Saito, A. *Inorg. Chim. Acta* **1990**, *171*, 135−137. (b) Himeno, S.; Takamoto, M.; Higuchi, A.; Maekawa, M. *Inorg. Chim. Acta* **2003**, *348*, 57−62. (c) Miras, H. N.; Ochoa, M. N. C.; Long, D.-L.; Cronin, L. *Chem. Commun.* **2010**, *46*, 8148−8150. (d) Miras, H. N.; Stone, D.; Long, D.-L.; McInnes, E. J. L.; Kogerler, P.; Cronin, L. *Inorg. Chem.* **2011**, *50*, 8384−8391. (e) Miras, H. N.; Sorus, M.; Hawkett, J.; Sells, D. O.; McInnes, E. J. L.; Cronin, L. J. *J. Am. Chem. Soc.* **2012**, *134*, 6980−6983.

(19) (a) Ueda, T.; Wada, K.; Hojo, M. *Polyhedron* **2001**, *20*, 83−89. (b) Ueda, T.; Komatsu, M.; Hojo, M. *Inorg. Chim. Acta* **2003**, *344*, 77−84.

(20) Ueda, T.; Nambu, J.; Yokota, H.; Hojo, M. *Polyhedron* **2009**, *28*, 43−48.

(21) (a) Himeno, S.; Osakai, T.; Saito, A.; Hori, T. *Bull. Chem. Soc. Jpn.* **1992**, *65*, 799−804. (b) Himeno, S.; Takamoto, M.; Hoshiba, M.; Higuchi, A.; Hashimoto, M. *Bull. Chem. Soc. Jpn.* **2004**, *77*, 519−524.

(22) Sheldrick, G. M. *Acta Crystallogr.* **2008**, *A64*, 112−122.

(23) Least-squares function is minimized as follows: $\sum w(F_o^2 - F_c^2)^2$, where w = least-squares weighting.

(24) The standard deviation of an observation with unit weighing is given as $[\sum w(F_o^2 - F_c^2)^2/(N_o - N_v)]^{1/2}$, where N_o = number of observations and N_v = number of variables.

(25) Flack, H. D. *Acta Crystallogr.* **1983**, *A39*, 876−881.

(26) Cromer, D. T.; Waber, J. T. *International Tables for X-ray Crystallography*; Kynoch Press: Birmingham, England, 1974; Vol. *IV*, Table 2.2 A.

(27) Ibers, J. A.; Hamilton, W. C. *Acta Crystallogr.* **1964**, *17*, 781−782.

(28) Creagh, D. C.; McAuley, W.J. *International Tables for Crystallography*; Wilson, A. J. C., Ed.; Kluwer Academic Publishers: Boston, MA, 1992; Vol. *C*, pp 219−222, Table 4.2.6.8.

(29) The crystal-to-detector distance was 127.40 mm for 1-S_2VW_{17} and 127.00 mm for 4-S_2VW_{17}. The data were collected at a temperature of −150 + 1 °C to a maximum 2θ value of 55.0°. A total of 120 oscillation images were collected for 1-S_2VW_{17} or 760 for 4-S_2VW_{17}. A data sweep was done using ω scans from 0.0 to 180.0° in 3.0° step at χ = 45.0° and φ = 0.0° for 1-S_2VW_{17} and from 130.0 to 190.0° in 1.0° steps at χ = 45.0° and φ = 30.0° for 4-S_2VW_{17}. The exposure rate was 12.0 s/° for 1-S_2VW_{17} and 30.0 s/° for 4-S_2VW_{17}. A second sweep was performed using ω scans from 0.0 to 180.0° in 3.0° steps at χ = 45.0° and φ = 210.0° for 1-S_2VW_{17} and from 0.0 to 160.0° in 0.5° steps at χ = 45.0° and φ = 180.0° for 4-S_2VW_{17}. The exposure rate was 12.0 s/° for 1-S_2VW_{17} and 30.0 s/° for 4-S_2VW_{17}. Two more other sweeps were performed for 4-S_2VW_{17} only. One was done using ω scans from 130.0 to 190.0° in 1.0° steps at χ = 45.0° and φ = 100.0°, where the exposure rate was 30.0 s/°, and another one was done using ω scans from 0.0 to 160.0° in 0.5° steps at χ = 45.0° and φ = 250.0°, where the exposure rate was 30.0 s/°. Readout was performed in the 0.100 mm pixel mode. Of the 91 799 reflections for 1-S_2VW_{17} and 202 709 for 4-S_2VW_{17} that were collected, 16 048 and 26 479 were unique (R_{int} = 0.0458 and 0.0383), respectively; equivalent reflections were merged. The linear absorption coefficient, μ, for Mo Kα radiation is 170.556 cm^{-1}. An empirical absorption correction was applied, which resulted in transmission factors ranging from 0.169 to 0.495 for 1-S_2VW_{17} and from 0.143 to 0.256 for 4-S_2VW_{17}. The data were corrected for Lorentz and polarization effects.

(30) Wertz, J. E.; Orton, J. W.; Auzins, P. *Discuss. Faraday Soc.* **1961**, *31*, 140−150.

(31) Hanson, G. R.; Gates, K. E.; Noble, C. J.; Grifffin, M.; Benson, S. *J. Inorg. Biochem.* **2004**, *98*, 903−916.

(32) Ueda, T.; Nambu, J.; Lu, J.; Guo, S.-X.; Li, Q.; Martin, L. L.; Bond, A. M. *Dalton Trans.* **2014**, *43*, 5462−5473.

(33) Rocchiccioli-Deltcheff, C.; Fournier, M.; Franck, R.; Thouvenot, R. *Inorg. Chem.* **1983**, *22*, 207−216.

(34) Harmalker, S. P.; Leparulo, M. A.; Pope, M. T. *J. Am. Chem. Soc.* **1983**, *105*, 4286−4292.

(35) Contant, R.; Abbessi, M.; Canny, J.; Belhouari, A.; Keita, B.; Nadjo, L. *Inorg. Chem.* **1997**, *36*, 4961−4967.

(36) Centi, G.; Perathoner, S.; Trifiro, F.; Aboukais, A.; Aissi, C. F.; Guelton, M. *J. Phys. Chem.* **1992**, *96*, 2617−2629.

(37) Nambu, J.; Ueda, T.; Guo, S.-X.; Boas, J. F.; Bond, A. M. *Dalton Trans.* **2010**, *39*, 7364−73.

(38) McGarvey, B. R. *J. Phys. Chem.* **1967**, *71*, 51−66.

(39) (a) Smith, D. P.; Pope, M. T. *Inorg. Chem.* **1973**, *12*, 331−336. (b) Altenau, J. J.; Pope, M. T.; Prados, R. A.; So, H. *Inorg. Chem.* **1975**, *14*, 417−421. (c) Himeno, S.; Osakai, T.; Saito, A. *Bull. Chem. Soc. Jpn.* **1991**, *64*, 21−28.

(40) (a) Abbessi, M.; Contant, R.; Thouvenot, E.; Herve, G. *Inorg. Chem.* **1991**, *30*, 1695−1702. (b) Keita, B.; Girard, F.; Nadjo, L.; Contant, R.; Canny, J.; Richet, M. *J. Electroanal. Chem.* **1999**, *478*, 76−82. (c) Keita, B.; Mbomekalle, I. M.; de Oliveira, P.; Ranjbari, A.; Justum, Y.; Nadjo, L.; Pompon, D. *J. Cluster Sci.* **2006**, *17*, 221−233.